

## Analysis of underground stratification based on CPTu profiles using high-pass spatial filter

J. Rainer<sup>1</sup> H. Szabowicz<sup>2</sup>

<sup>1</sup>Wroclaw University of Science and Technology. Email: [kubarainer@gmail.com](mailto:kubarainer@gmail.com)

<sup>2</sup>Wroclaw University of Science and Technology. Email: [hubert.szabowicz@gmail.com](mailto:hubert.szabowicz@gmail.com)

**Abstract:** This paper discusses the issue of underground stratification based on cone penetration tests (CPTu) using high-pass spatial filters. The first part of this article is a general characteristic of cone penetration tests. The basic classification systems were described, only two of them were used in algorithm. Next, basic definitions and concepts concerning digital image processing and high-pass spatial filters were introduced. Then an algorithm that uses high-pass spatial filters for stratification analysis of underground soil structure was provided. The final part of this article contains results and conclusions from the analysis carried out on datasets provided as required for TC304 Student Contest on Spatial Data Analysis (September 22, 2019, Hannover, Germany).

**Keywords:** Cone Penetration Test, Underground Stratification Analysis, Digital Image Processing, High-Pass Spatial Filter

### 1. Introduction

The most important part in the whole process of designing of the foundation is to recognize the subgrade properly. One of the testing in situ method uses in geotechnics to investigate the underground structure is the cone penetration test (Rybak and Stilger-Szydło 2010). CPTu owes its popularity to simplicity and quickness of carrying out tests. Obtained results can be used for instance to determine soil layers in geological profiles.

#### 1.1 General characteristic of cone penetration tests

The cone penetration test (CPTu) involves pushing a penetration rod with a special cone into the ground. The velocity of penetration is constant and shall be around 20 mm/s. During penetration, test values of the resistance under the tip of the cone  $q_t$ , local skin friction on the sleeve of the cone  $f_s$  and the pore pressure in three points  $u_1, u_2, u_3$  can be measured. The measured values data is sent to a computer in constant time cycles. Nowadays, it can even be 2 times per second which corresponds to recording profile every 1 cm. Therefore, such sampling may be regarded as a quasi-continuous measure.

The record can be distorted due to geometric properties of the cone, atmospheric pressure and pore water pressure. The normalized cone resistance  $Q_{tn}$  and normalized sleeve friction  $F_r$

had been implemented to reduce the impact of disturbances caused by geometric properties of the cone (Robertson 1990).

$$Q_{tn} = \frac{q_t - \sigma_{v0}}{P_a} \cdot C_N \quad (1)$$

$$F_r(\%) = 100 \cdot \frac{f_s}{q_t - \sigma_{v0}} \quad (2)$$

where  $P_a = 101.3kPa$  is one atmosphere of pressure,  $\sigma'_{v0}$  and  $\sigma_{v0}$  are the effective and total overburden stress values, and  $C_N$  is the correction factor for the effective overburden stress:

$$C_N = \min[(P_a/\sigma'_{v0})^n; 1,7] \quad (3)$$

The exponent  $n$  should be calculated iteratively according to the following formula (Robertson 2009):

$$n = \min \left[ 0,381 \cdot I_c - 0,05 \cdot \frac{P_a}{\sigma'_{v0}} - 0,15; 1,0 \right] \quad (4)$$

where  $I_c$  is the soil behaviour type (SBT) index according to Robertson and Wride:

$$I_c = \sqrt{[3,47 - \log Q_{tn}]^2 + [1,22 + \log F_r]^2} \quad (5)$$

Very important parameters in different interpretations are friction ratio  $R_f$  and pore pressure parameter  $B_q$ :

$$R_f(\%) = \frac{f_s}{q_t} \cdot 100 \quad (6)$$

$$B_q = \frac{u_2 - u_0}{q_t - \sigma_{v0}} \quad (7)$$

### 1.2 Soil behaviour type classification

A significant element of the process of investigating the underground structure with the cone penetration test is the interpretation of obtained results. One shall remember that tests, even if they are perfectly made, can be useless when interpretation is poorly managed. The essential use of the cone penetration tests is to classify soil behavior type based on normalized measurement parameters. There are many examples of nomograms which allow for identification of the soil behaviour type. One of the main widely used methods is Robertson's classification form 1986.

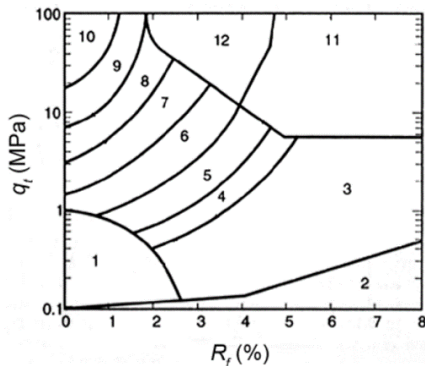


Figure 1. Roberson soil behaviour type classification chart (Robertson 1986)

The Roberson's chart in Figure 1. rest on the relation between tip resistance  $q_t$  and friction ratio  $R_f$ . The area of the nomogram has been divided into 12 soil behaviour types (SBT) parts. According to where measured point is located the classification is made.

Table 1. Numbers of subdivisions and corresponding Soil Behaviour Types (Robertson 1986)

SBT	Soil behaviour type
1	Sensitive fine grained
2	Organic material
3	Clay
4	Silty clay to clay
5	Clayey silt to silty clay
6	Sandy silt to clayey silt
7	Silty sand to sandy silt
8	Sand to silty sand
9	Sand
10	Gravelly sand to sand
11	Very stiff fine grained
12	Sand to clayey sand

In 1990, Robertson developed and modified his classification. The new method is based on the normalized cone resistance  $Q_{tn}$  and normalized sleeve friction  $F_r$ . Robertson reduced the number of soil behaviour types to 9. In 2009, he updated the normalized cone resistance and related it to the SBT nomogram

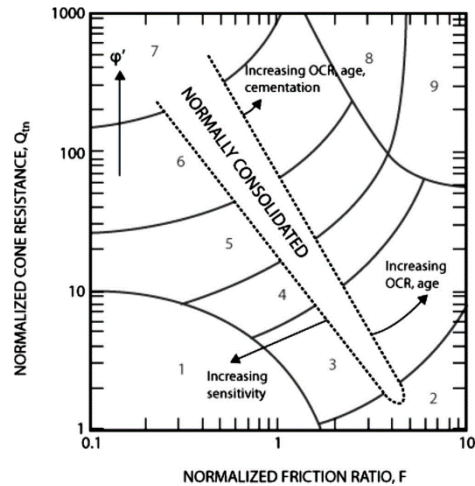


Figure 2. Roberson's soil behaviour type classification chart (Robertson 1990)

Table 2. Numbers of subdivisions and corresponding Soil Behaviour Types (Robertson 1990)

SBT	Soil behaviour type
1	Sensitive, fine grained
2	Organic soils- peats
3	Clays – silty clay to clay
4	Silt mixtures- clayey silt to silty clay
5	Sand mixtures- silty sand to sandy silt
6	Sand- clean sand to silty sand
7	Gravelly sand to dense sand
8	Very stiff sand to clayey sand
9	Very stiff, fine grained

It is possible to classify soil layers using the soil behaviour type index  $I_c$ . The value of the index increases as the main grain size is decreased. This method is based on Robertson's classification from 1990 except regions 1, 8 and 9.

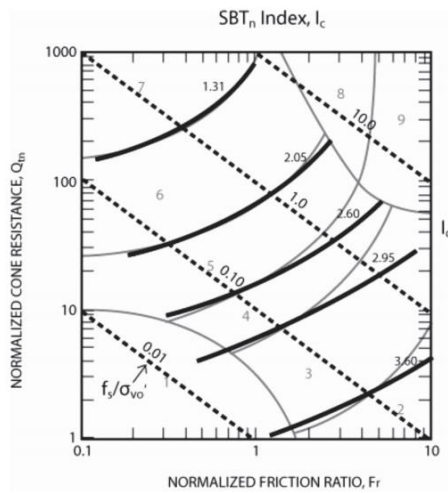


Figure 3. The  $I_c$  thresholds showed on Robertson's soil behaviour type classification chart (Robertson 2009)

Table 3. SBT index classification proposed by (Robertson and Wride 1998)

Classification	Soil behavior type index, $I_c$
SBT2	$I_c > 3,60$
SBT3	$2,95 \leq I_c < 3,60$
SBT4	$2,60 \leq I_c < 2,95$
SBT5	$2,05 \leq I_c < 2,60$
SBT6	$1,31 \leq I_c < 2,05$
SBT7	$I_c < 1,31$

### 1.3 Analysis of the impact of soil layering on the CPTu recordings

Cone penetration tests CPTu provide a lot of information which can be used to evaluate soil properties in the profile. But we should remember that the soil's response in the form of resistance in a specific point hinges on spatial arrangement of soil layers located above and below the cone. The reason of this fact can be illustrated by the analogy with behaviour of the foundation pile in the limit state (Lim Yi Xian 2017). The slip surfaces are crossing through the layers above and below the cone. This is the reason why the cone resistance  $q_t$  and the local skin friction  $f_s$  depend on the sequence and properties of all ground layers the impact zone of the pushing cone.

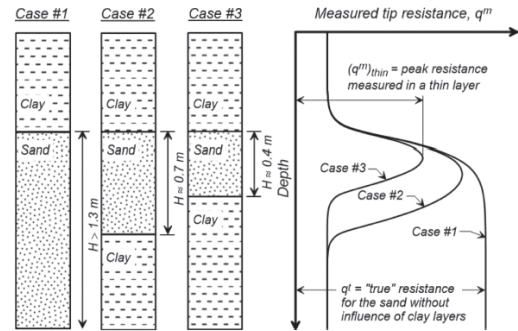


Figure 4. A schema of effect of thin layer of the sand included into a clay (Boulangier R.W. DeJong J.T., 2018)

The effect of different size layers inclusions is presented in Figure 4. The graph on the right side shows the measured tip resistance  $q_m$ . As can be seen, the value of  $q_m$  is increasing as the cone approaches the sand layer. And vice versa, when the cone tip is approaching the footwall of the sand layer, the tip resistance decreases. The 1st case presents the "true"  $q_t$  value which is free from the effect of thin layer. The transitional zone is defined as a range around the strata boundary where the value of the measured tip resistance  $q_m$  changes smoothly even though  $q_t$  change should be sudden. The effect of thin layer occurs when the peak  $q_m$  is lower than the corresponding value of  $q_t$ . In Figure 4. it can be seen that the thinner the layer, the larger the observational error is. Therefore, the clear designation of strata boundary is hampered, which in turn causes errors in reconnaissance and stratification. In order to improve interpretation of CPTu results, various mathematical operations can be used, such as high-pass spatial filters.

### 2. Characterisation of high-pass spatial filters

High-pass spatial filters are widely used in signal and image processing (Cristobal G. et al., 2011). This filter can be used to perform some modifications, enhancements or noise reductions on 1D or 2D signal. It is widely used to edge detection in pictures. The edge is defined as a point or line where a sudden change of the recorded value can be seen. In fact, there is always some transitional zone around the linear or nonlinear edge.

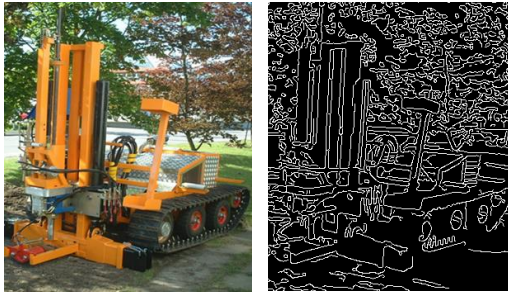


Figure 5. a) Original image, b) Image after high-pass filtering

In Figure 5., a high-pass spatial filter has been shown. In Figure 5b, the edges of the object presented in Figure 5a are visible. One of the basic high-pass filter is Laplacian. Laplacian is a differential operator given by the divergence of the gradient of a function on Euclidian space. In 2D space it is given by the formula:

$$\nabla^2 = \frac{\partial^2}{\partial x^2} + \frac{\partial^2}{\partial y^2} \quad (8)$$

This filter can detect edges defined by the largest rate of change of quantity, i.e. points where the gradient reaches its maximum value. An equivalent of Laplacian on the plane is the second derivative. Therefore, points of the maximum gradient are points where the second derivative is equal to zero. In case of the cone penetration test where record is a discrete signal, a finite difference can be used to replace the second derivatives in a Laplacian formula.

Another widely used filter in image processing is a Sobel operator. It is also a discrete differential operator which allows for approximation of the gradient of the image intensity function. This filter is less sensitive to noise in the signal due to the usage of the 3x3 kernels which are convolved with the original signal. The derivatives are calculated separately for horizontal and vertical changes with different kernels. Respectively, the vertical values for horizontal gradient are averaged, and for vertical gradient, the horizontal values are averaged.

### 3. The stratification procedure using a high-pass filter

The cone penetration test records can be treated as a signal and process in a similar manner as sound or image. The digital signal processing can be used. In order to make a stratification

algorithm, the original idea based on a high-pass filter has been used. In order to increase the probability of correct stratification, the calculation algorithm is based on two different soil behaviour type classification methods. The Robertson's soil behaviour type classification chart (1990) and the SBT index classification were used. Both classification results are shown. If the soil behaviour types for both methods are different, then the Robertson's SBT classification (1990) shall be accepted as more reliable.

#### 3.1. Step I – import and calculation of the basic parameters

During the first step, the tip resistance  $q_t$ , sleeve friction  $f_s$ , the effective  $\sigma'_{v0}$  and total overburden  $\sigma_{v0}$  stresses shall be provided. Next, the normalized parameters  $Q_{tn}$ ,  $F_r$  and soil behaviour type index  $I_c$  can be calculated.

#### 3.2. Step II – changing 1D signal into a 2D image

Since Sobel operator is working only for 2D objects, the 1D CTPu signal in the form of the n elements list should be extended to the n x 3 matrix. Then, for the needs of the depiction data in grayscale, every matrix is normalized by dividing by the maximal value of itself (making a 0 to 1 scale). The white colour is assigned to the maximum value and the black to the minimum. Intermediate values have a grayscale. The image of the CPTu record is presented in the form of horizontal monochromatic lines (Figure 5. a) and b)).

#### 3.3. Step III – high-pass filtering of the recording image

The further step is to use the high-pass filter on the recording image to detect the edges. In this computational algorithm, the Sobel operator was used. Because the signal was extended by duplicating the values in the horizontal direction, the gradient in this line is always equal to zero. Increasing the dimension does not impact the edge detection. In the output data of the filter, the matrix components are equal to 1 when edge is detected and are equal to 0 where it is not. After filtering, edges can be seen as horizontal white lines.

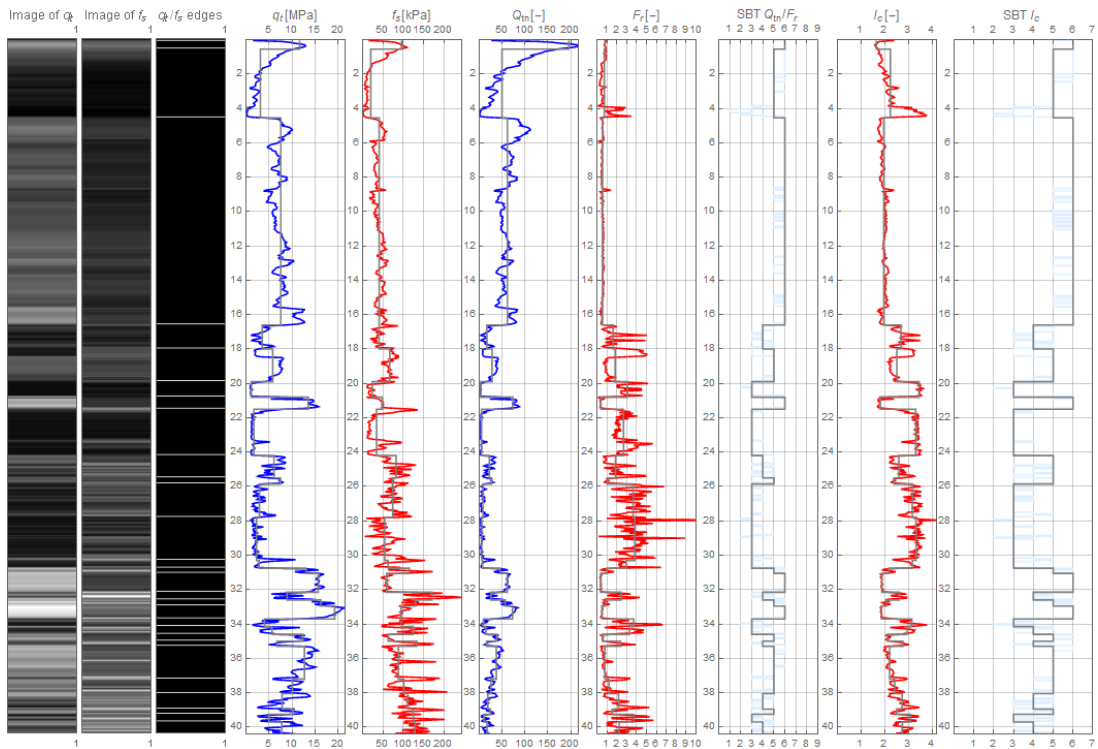


Figure 5. Results of using the computing algorithm on the training dataset: a) Image of  $q_t$ , b) Image of  $f_s$ , c) Image of  $q_t/f_s$  edges, CPTu records of: d)  $q_t$  and e)  $f_s$  with averaged values, computed values of: f)  $Q_{tn}$  and g)  $F_r$  with averaged values, h) Soil Behaviour Type according to Robertson (1990), i) computed values of  $I_c$  for every point in profile and averaged after filtering, j) Soil Behaviour Type according to  $I_c$  index

### 3.4. Step IV – defining the strata boundary according to detected edges

In the case of SBT index classification, since the computing algorithm operates only on one parameter, the strata boundaries are strictly defined by detected edges. But as regards Robertson's classification (1990), two variables  $Q_{tn}$  and  $F_r$  should be used. Because the image of the primary dataset  $q_t$  and  $f_s$  can be different from the normalized  $Q_{tn}$  and  $F_r$  the edge detection is made on unmodified parameters. In the images of  $q_t$  and  $f_s$  after using Sobel operator, the edges do not always appear in the same locations. It is assumed that the strata boundary occurs only when the edges are close to each other in both images. This occurs because, during the measurement, the sleeve is placed a few centimetres above the cone tip (maximum 10 cm). Therefore, the difference between the edges detected for  $q_t$  and  $f_s$  cannot exceed 10 cm.

If detected edges are closer to each other than 10 cm, the strata boundary is placed in the  $q_t$  edge but if it is further away, the boundary cannot be accepted (Figure 5. c).

### 3.5. Step V – calculation of the average parameter values within the layer

After defining the strata boundary in the geological profile using the images, the normalized parameters can be used again. The representative parameters are equal to the average value within the layer. The transitional effects are taken into consideration by rejecting the values located closer to the edges than 10 cm.  $Q_{tn}$  and  $F_r$  are presented in Figure 5. f) and g).

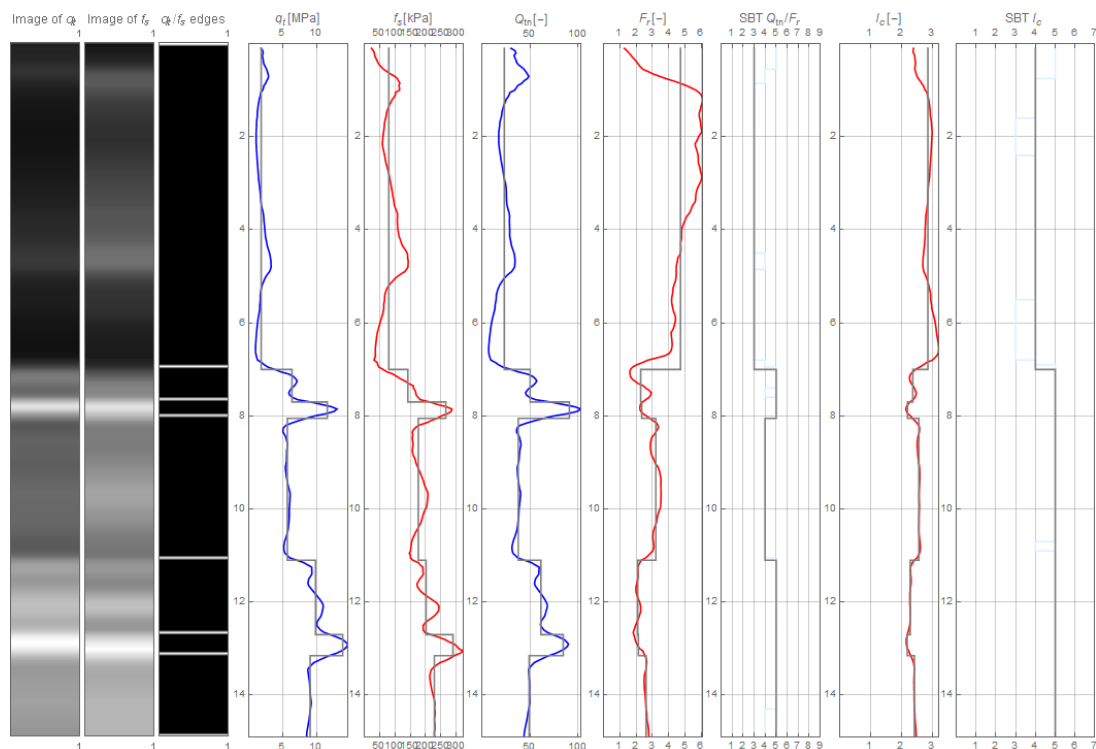


Figure 6. Results of using the computing algorithm on the testing dataset #1: a) Image of  $q_t$ , b) Image of  $f_s$ , c) Image of  $q_t/f_s$  edges, CPTu records of: d)  $q_t$  and e)  $f_s$  with averaged values, computed values of: f)  $Q_{tn}$  and g)  $F_r$  with averaged values, h) Soil Behaviour Type according to Robertson (1990), i) computed values of  $I_c$  for every point in profile and averaged after filtering, j) Soil Behaviour Type according to  $I_c$  index

### 3.6. Step VI – soil behaviour type classification

The further step is to classify the soil behaviour type based on the averaged normalized parameters for Robertson (1990) (Figure 5. h) and averaged  $I_c$  for the SBT index classification (Figure 5. j)).

### 3.7. Step VII – comparison of both classifications

The last stage of the stratification procedure is to compare the obtained results. If both classifications are coinciding, then it is accurate to accept it. But if they are different, the Robertson classification (1990) shall be used as more reliable.

## 4. Results of the analysis of the data provided as required for TC304 Student Contest on Spatial Data Analysis

The computing algorithm was verified for the training data set provided for the Contest. The

results are presented in point 3. In this example, the algorithm has been introduced.

The stratification and classification results are similar for both methods based on  $Q_{tn}/F_r$  and on  $I_c$ . The soil behaviour type is almost always the same for the testing datasets. The strata boundaries are identified close for both classifications. The calculations on the testing datasets are presented in Figure 6., Figure 7. and Figure 8.

## 5. Conclusions

The results of stratification with high-pass filtering may be considered as reliable. The identified layers are reasonable. The thin layers do not appear and the variability of SBT classification is minor. Because of the stratification and averaging, the measurement is

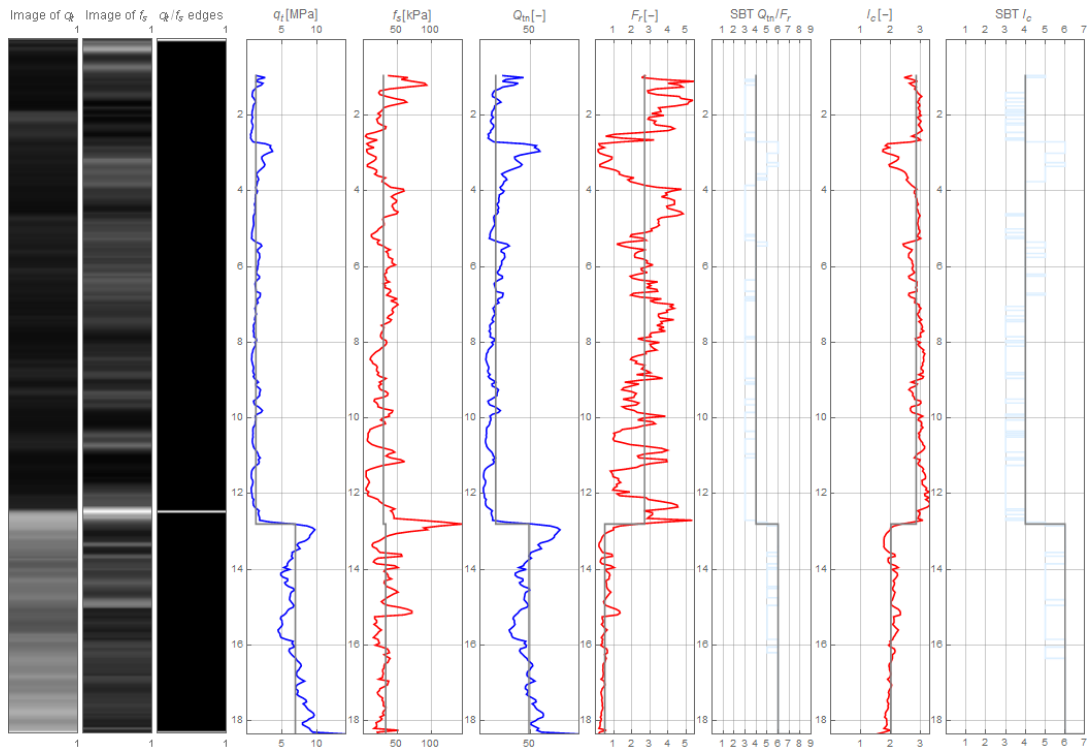


Figure 7. Results of using the computing algorithm on the testing dataset #2: a) Image of  $q_t$ , b) Image of  $f_s$ , c) Image of  $q_t/f_s$  edges, CPTu records of: d)  $q_t$  and e)  $f_s$  with averaged values, computed values of: f)  $Q_{tn}$  and g)  $F_r$  with averaged values, h) Soil Behaviour Type according to Robertson (1990), i) computed values of  $I_c$  for every point in profile and averaged after filtering, j) Soil Behaviour Type according to  $I_c$  index

getting less sensitive to the background noise, which is equivalent to the large number of thin layers. In addition, the averaged values correctly represent the actual records. When comparing the stratification provided by the contest organizer and the results for the training dataset obtained with high-pass filter, the form of the stratification seems to be similar. The uniqueness of this algorithm is based on an assumption that the CPTu record can be treated as a signal and next as an image in order to use the digital image processing functions. The obtained results can be used to the further analysis of the subgrade like the spatial variability within the separated layers (Puła, Bagińska, Kawa 2017)

## References

Boulander R.W. DeJong J.T., 2018 *Inverse filtering procedure to correct cone penetration data for thin-layer and transition effects*. *Cone penetration testing 2018: proceeding of the 4th*

*International Symposium on Cone Penetration Testing*, Delft, The Netherlands

Cristobal G.et al., 2011, *Optical and digital image processing: Fundamentals and applications*, Wiley- VCH Verlag GmbH&Co

Lim Yi Xian, 2017, *Numerical study of cone penetration test in clays using press-replace method*, Ph.D Theses, China

Robertson et al. 1986, *Use of piezometer cone data IN-SITU'86*, *ASCE Speciality Conference*

Robertson, P.K. 1990. *Soil classification using the cone penetration test*. *Canadian Geotechnical Journal*,

Robertson, P.K. 2009. *Interpretation of cone penetration tests – a unified approach*. *Canadian Geotechnical Journal*, 46, 1337-1355. 27, 151-158.

Robertson, P. (1998). *Evaluating cyclic liquefaction potential using the cone*

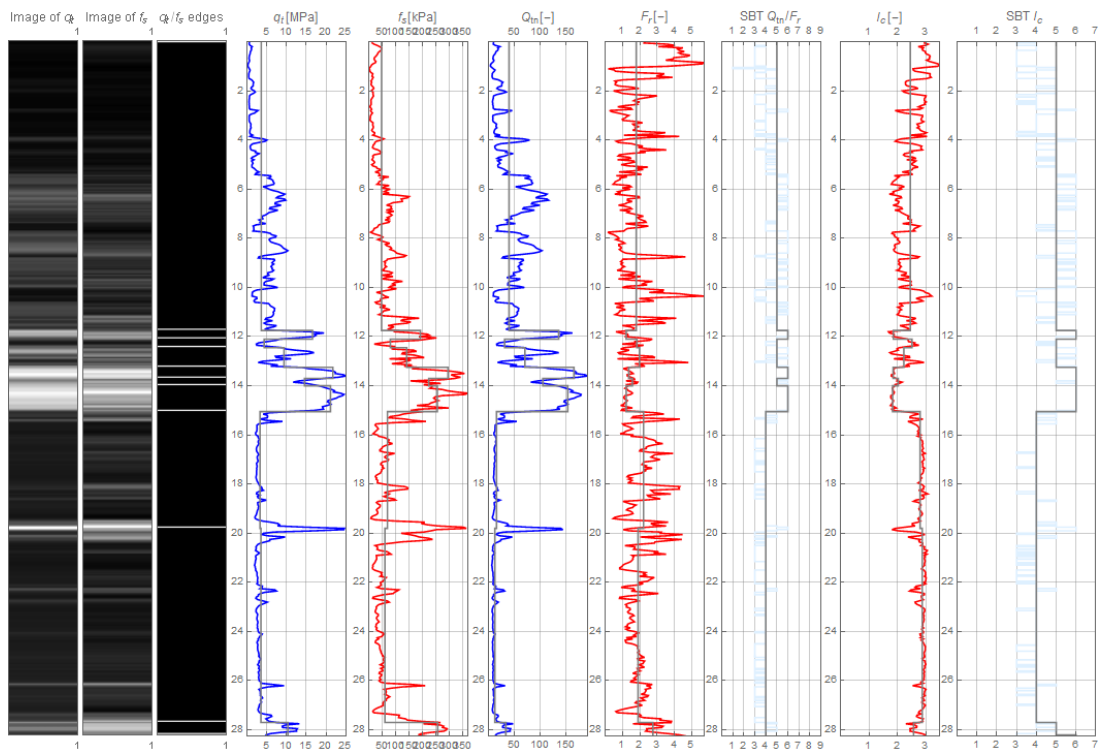


Figure 8. Results of using the computing algorithm on the testing dataset #3: a) Image of  $q_t$ , b) Image of  $f_s$ , c) Image of  $q_t/f_s$  edges, CPTu records of: d)  $q_t$  and e)  $f_s$  with averaged values, computed values of: f)  $Q_{tn}$  and g)  $F_r$  with averaged values, h) Soil Behaviour Type according to Robertson (1990), i) computed values of  $I_c$  for every point in profile and averaged after filtering, j) Soil Behaviour Type according to  $I_c$  index

*penetration test.* Canadian Geotechnical Journal - CAN GEOTECH J. 35. 442-459.

Rybak, J., and Stilger-Szydło, E. 2010, *The importance and faults of subgrade reconnaissance in foundations of land transport*, Nowoczesne Budownictwo Inżynieryjne

Puła, W., Bagińska, I., Kawa, M., Pieczynska-Kozłowska, J. 2017, *Estimation of spatial variability of soil properties using CPTu results: a case study*, Conference: 6th International Workshop „In-situ and laboratory characterization of OC subsoil”